



ELSEVIER

26 September 1996

PHYSICS LETTERS B

Physics Letters B 385 (1996) 479–486

# Precision measurements of antiproton-proton forward elastic scattering parameters in the 3.7 to 6.2 GeV/c region

Fermilab E760 Collaboration

T.A. Armstrong<sup>f</sup>, D. Bettoni<sup>b</sup>, V. Bharadwaj<sup>a</sup>, C. Biino<sup>g</sup>, G. Blanford<sup>d</sup>, G. Borreani<sup>g</sup>, D. Broemmelsiek<sup>d</sup>, A. Buzzo<sup>c</sup>, R. Calabrese<sup>b</sup>, A. Ceccucci<sup>g</sup>, R. Cester<sup>g</sup>, M. Church<sup>a</sup>, P. Dalpiaz<sup>b</sup>, P.F. Dalpiaz<sup>b</sup>, R. Dibenedetto<sup>g</sup>, D. Dimitroyannis<sup>e</sup>, M. Fabbri<sup>b</sup>, J. Fast<sup>d</sup>, A. Gianoli<sup>b</sup>, C.M. Ginsburg<sup>e</sup>, K. Gollwitzer<sup>d</sup>, G. Govi<sup>g</sup>, A. Hahn<sup>a</sup>, M.A. Hasan<sup>f</sup>, S. Hsueh<sup>a</sup>, R. Lewis<sup>f</sup>, E. Luppi<sup>b</sup>, M. Macrí<sup>c</sup>, A.M. Majewska<sup>f</sup>, M. Mandelkern<sup>d</sup>, F. Marchetto<sup>g</sup>, M. Marinelli<sup>c</sup>, J. Marques<sup>d</sup>, W. Marsh<sup>a</sup>, M. Martini<sup>b</sup>, M. Masuzawa<sup>e</sup>, E. Menichetti<sup>g</sup>, A. Migliori<sup>g</sup>, R. Mussa<sup>g</sup>, S. Palestini<sup>g</sup>, M. Pallavicini<sup>c</sup>, S. Passagio<sup>c</sup>, N. Pastrone<sup>g</sup>, C. Patrignani<sup>c</sup>, T.K. Pedlar<sup>e</sup>, J. Peoples Jr.<sup>a,e</sup>, L. Pesando<sup>g</sup>, F. Petrucci<sup>b</sup>, M.G. Pia<sup>c</sup>, S. Pordes<sup>a</sup>, P.A. Rapidis<sup>a</sup>, R. Ray<sup>e,a</sup>, J. Reid<sup>f</sup>, G. Rinaudo<sup>g</sup>, E. Robutti<sup>c</sup>, B. Rocuzzo<sup>g</sup>, J. Rosen<sup>e</sup>, A. Santroni<sup>c</sup>, M. Sarmiento<sup>e</sup>, M. Savrié<sup>b</sup>, J. Schultz<sup>d</sup>, K.K. Seth<sup>e</sup>, A. Smith<sup>d</sup>, G.A. Smith<sup>f</sup>, M. Sozzi<sup>g</sup>, S. Trokenheim<sup>e</sup>, M.F. Weber<sup>d</sup>, S. Werkema<sup>a</sup>, Y. Zhang<sup>f</sup>, J. Zhao<sup>e</sup>, G. Zioulas<sup>d</sup>

<sup>a</sup> Fermi National Accelerator Laboratory, Batavia, Illinois 60510, USA

<sup>b</sup> Istituto Nazionale di Fisica Nucleare and University of Ferrara, 44100 Ferrara, Italy

<sup>c</sup> Istituto Nazionale di Fisica Nucleare and University of Genoa, 16146 Genoa, Italy

<sup>d</sup> University of California at Irvine, California 92717, USA

<sup>e</sup> Northwestern University, Evanston, Illinois 60208, USA

<sup>f</sup> Pennsylvania State University, University Park, Pennsylvania 16802, USA

<sup>g</sup> Istituto Nazionale di Fisica Nucleare and University of Turin, 10125 Turin, Italy

Received 26 July 1996

Editor: L. Montanet

## Abstract

Differential cross sections for  $\bar{p}p$  elastic scattering have been measured for very small momentum transfers at six different incident antiproton momenta in the range 3.7 to 6.2 GeV/c by the detection of recoil protons at scattering angles close to 90°. Forward scattering parameters  $\sigma_T$ ,  $b$ , and  $\rho$  have been determined. For the  $\rho$ -parameter, up to an order of magnitude higher level of precision has been achieved compared to that in earlier experiments. It is found that existing dispersion theory predictions are in disagreement with our results for the  $\rho$ -parameter.

PACS: 13.75.Cs; 11.55.Fv

There is no general formalism which permits calculation of hadron-hadron elastic scattering. Forward angle, or zero momentum transfer ( $\sqrt{|t|} = 0$ ) elastic scattering amplitudes,  $f_n(0)$  can, however, be related to total cross sections,  $\sigma_T$  by the application of the principles of unitarity, analyticity, and crossing symmetry, which are collectively embodied in the dispersion theory. Unitarity leads to the well-known optical theorem

$$\text{Im } f_n(0) = k_{\text{cm}} \sigma_T / 4\pi \quad (1)$$

Analyticity and crossing symmetry, which dictate that  $f_n(0)$  for both particle-particle and particle-antiparticle elastic scattering arise from the same analytic amplitudes, enable dispersion theory to predict  $\text{Re } f_n(0)$ . For  $\bar{p}p$  scattering dispersion relations predict  $\rho$ , defined as

$$\rho \equiv \text{Re } f_n(0) / \text{Im } f_n(0), \quad (2)$$

at any given energy in terms of the integrals over  $\text{Im } f_n(0)$  for  $\bar{p}p$  and  $pp$  scattering at all energies, in the physical region ( $\sqrt{s} > 2m_p$ ) and the unphysical region ( $\sqrt{s} < 2m_p$ ). Since the parameters associated with the unphysical region are not directly measurable, measurements of  $\rho$  in the low energy region provide the most sensitive means of gaining knowledge about them. In this letter we report on the measurements of  $\bar{p}p$  elastic scattering differential cross sections at very small  $t$  at six momenta in the region 3.7 to 6.2 GeV/c and present results of their analysis to obtain forward scattering parameters.

Antiproton-proton elastic scattering can be described in terms of the Coulomb and nuclear amplitudes,  $f_c$  and  $f_n$ . Using the conventional parameterization of the nuclear amplitude at small  $t$ , one obtains

$$\frac{d\sigma}{dt} = \frac{\pi}{k^2} |f_c e^{i\delta} + f_n|^2 = \frac{d\sigma_c}{dt} + \frac{d\sigma_{\text{int}}}{dt} + \frac{d\sigma_n}{dt}, \quad (3)$$

$$\text{where } \frac{d\sigma_c}{dt} = \frac{4\pi\alpha_{\text{EM}}^2 G^4(t) (\hbar c)^2}{\beta^2 t^2}, \quad (4)$$

$$\frac{d\sigma_{\text{int}}}{dt} = \frac{\alpha_{\text{EM}} \sigma_T}{\beta |t|} G^2(t) e^{-\frac{1}{2} b |t|} (\rho \cos \delta + \sin \delta), \quad (5)$$

$$\text{and } \frac{d\sigma_n}{dt} = \frac{\sigma_T^2 (1 + \rho^2) e^{-b |t|}}{16\pi (\hbar c)^2}. \quad (6)$$

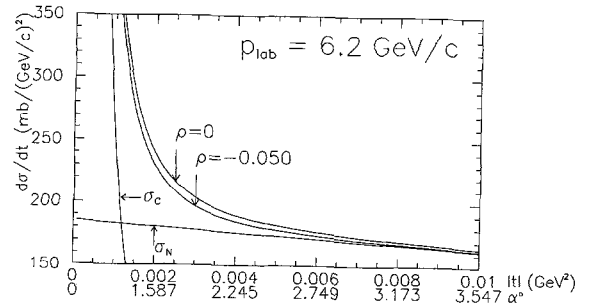


Fig. 1. Partial and total  $\bar{p}p$  differential elastic scattering cross sections as calculated for typical values of  $\sigma_T$ ,  $b$  and  $\rho$ . The zero of the ordinate has been suppressed to make the difference between the cross sections for  $\rho = 0$  and  $\rho = -0.05$  visible.

Here,  $\alpha_{\text{EM}}$  is the fine structure constant. The proton dipole form factor  $G(t) = (1 + \Delta)^{-2}$ , with  $\Delta \equiv |t|/0.71 \text{ (GeV/c)}^2$ . The Coulomb phase [1],

$$\delta(t) = \alpha_{\text{EM}} \left[ 0.577 + \ln \left( \frac{b|t|}{2} + 4\Delta \right) + 4\Delta \ln(4\Delta) + 2\Delta \right]. \quad (7)$$

The Coulomb cross section is thus a known function of  $t$ . The nuclear and interference cross sections involve the parameters  $\sigma_T$ ,  $b$  and  $\rho$ , which must be determined experimentally.

Fig. 1 illustrates the different contributions to the differential cross section for a typical case. It is clear from this figure that in order to determine from the data all three parameters of forward scattering,  $\sigma_T$ ,  $b$ , and  $\rho$ , independently, it is necessary to measure relative cross sections accurately in an extended range of small  $t$ . The measurement should range from  $|t| > 0.015 \text{ (GeV/c)}^2$  (where the slope parameter  $b$  is best determined), past the Coulomb-nuclear interference region,  $|t| \approx 0.001 \text{ (GeV/c)}^2$  (where the  $\rho$  parameter has its maximum effect), to deep into the Coulomb region,  $|t| \leq 0.0001 \text{ (GeV/c)}^2$ , where the Coulomb cross section is  $> 95\%$  of the total, and can provide accurate absolute normalization. Further, the relative differential cross sections as well as  $t$  should be measured throughout the range with a precision of 1% or better.

Our measurements of the differential cross sections are based on the detection of proton recoils which correspond to antiproton scattering at extreme forward angles. The laboratory kinetic energy,  $T_p$ , of the recoil

protons and the recoil angle,  $\alpha$  (as measured from the perpendicular to the beam direction), are related to  $t$ ,

$$-t = 2m_p T_p = \frac{4m_p^2 \sin^2 \alpha}{(1/\beta_{cm}^2) - \sin^2 \alpha}, \quad (8)$$

where  $(1/\beta_{cm}^2) = (E_{beam} + m_p)/(E_{beam} - m_p)$ . Note that both  $t$  and  $T_p$  are to a very good approximation proportional to  $\alpha^2$ . The recoil measurement technique has been used before [2]. It has several important advantages over measurements of scattered antiprotons at small forward angles, the most important being that the problem of distinguishing elastically scattered antiprotons from non-interacting, or transmitted, antiprotons is avoided. Further, proton recoils have small energies and they can be detected with excellent energy resolution and signal to noise ratio in solid state detectors of modest thickness. For example, for  $|t|$  as large as  $0.04 (\text{GeV}/c)^2$ ,  $T_p \leq 22 \text{ MeV}$ , and recoil protons have a range of  $< 3000 \mu\text{m}$  in silicon. Finally, recoil protons corresponding to antiprotons scattered in a small cone at forward angles can be spread over a much larger azimuthal ring. Their detection in a device with only a small extension in  $\phi$  reduces problems associated with large count rates which are present at forward angles.

The measurements reported here were made in conjunction with Fermilab experiment E760. This experiment is located at the Antiproton Accumulator ring and is devoted to high resolution studies of charmonium states formed in antiproton-proton annihilation. The circulating antiproton beam in the accumulator ring (typically  $4 \times 10^{11} \bar{p}$ ) intersects an internal  $\text{H}_2$  gas jet target (typically of density  $3.5 \times 10^{13}$  protons/cm<sup>2</sup>) to provide a  $\bar{p}p$  luminosity of about  $1 \times 10^{31} \text{ cm}^{-2} \text{ s}^{-1}$ . The interaction region consists of the intersection of a  $\sim 8 \text{ mm}$  diameter cylindrical beam with a  $\sim 7 \text{ mm}$  diameter gas jet. Charmonium resonances ( $\eta_c, J/\psi, ^1P_1, \chi_2, \eta'_c$  and  $\psi'$ ) were scanned by varying the momentum of the antiprotons in the range 3.5–6.2 GeV/c, and electromagnetic final states were detected in the E760 detector system, which has been described elsewhere [3]. The apparatus used for the measurements of the forward scattering parameters was incorporated in the luminosity monitor designed for the charmonium experiment. Elastic scattering data were only taken at the  $\bar{p}$  momenta corresponding to the masses of the charmonium

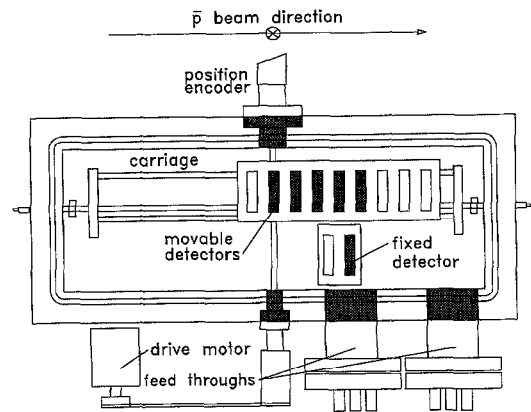
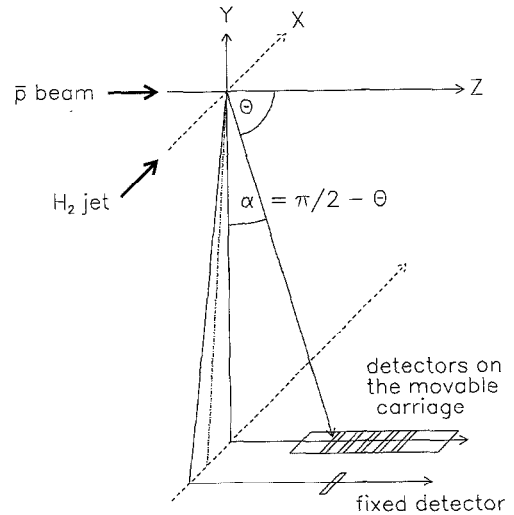


Fig. 2. (Top:) Schematic of the geometry of the apparatus for detecting recoil protons. (Bottom:) The detector pan.

resonances studied. The perturbation caused by charmonium resonances on the elastic scattering parameters is expected to be entirely negligible because the cross sections for resonant  $\bar{p}p \rightarrow (c\bar{c})_R \rightarrow \bar{p}p$  reactions are known to be five to seven orders of magnitude smaller than the  $\bar{p}p$  elastic scattering cross sections.

The geometry of the luminosity monitor is schematically illustrated in Fig. 2(a). The details of its construction and calibration have been described elsewhere [4]. Briefly, it consists of a 150 cm long tapered vacuum chamber suspended vertically from the beam

pipe such that a bank of solid state detectors in a pan at its bottom can “see” the  $\bar{p}p$  intersection region at recoil angles  $\alpha = 0^\circ$  to  $7^\circ$ . The detector pan (Fig. 2(b)) had one fixed detector at  $\alpha = 3.547(6)^\circ$  for luminosity measurements using known forward scattering parameters, and five detectors (at nominal positions of  $\alpha = 1^\circ, 2^\circ, \dots, 5^\circ$ ) on a movable carriage to independently determine the scattering parameters by analyzing the detailed shape of the measured differential cross sections. The carriage could be moved by remote control to bring the detectors to any desired recoil angle from  $\alpha_{\text{nominal}}$  to  $\alpha_{\text{nominal}} - 7^\circ$ . The silicon detectors were of active area  $\sim 1 \text{ cm} \times 5 \text{ cm}$  and depletion depths of either  $500 \mu\text{m}$  or  $3000 \mu\text{m}$ . A thin  $^{244}\text{Cm}$  alpha source could be inserted by remote control to a position over the detectors at  $\approx 100 \text{ cm}$  height to allow in situ calibrations of energy and relative solid angle.

In the recoil method the experimental problem consists of making precision measurements of the energies of the recoil protons and their relative yield at different recoil angles. In the present experiment the recoil angles typically ranged from  $\alpha \approx 1.1^\circ (\pm 0.35^\circ)$  to  $5^\circ (\pm 0.35^\circ)$  which at  $5 \text{ GeV}/c$  correspond to  $|t| \approx 0.0009 (\pm 0.0005)$  to  $|t| \approx 0.019 (\pm 0.0024)$   $(\text{GeV}/c)^2$  where the  $\pm$  numbers indicate the approximate acceptance in  $\alpha$  and  $t$  due to the finite geometry of the detectors and the interaction region. The range of recoil energies was  $T_p \approx 0.4$  to  $11 \text{ MeV}$ . Since five different detectors on the movable carriage were used to cover the full range of recoil angles, it was necessary that the relative solid angles which they subtend at the interaction region and their individual energy calibrations be determined accurately. This was done repeatedly during the course of the measurements by inserting the remotely controlled  $^{244}\text{Cm}$  alpha source in position above the detectors, when no beam was circulating. The details of detector performance and relative solid angle measurements have been presented elsewhere [4]. In summary, the different detectors had energy resolutions between  $60$  and  $110 \text{ keV}$ , and throughout the measurements their energy and effective area calibrations were found to be reproducible to within  $0.2\%$  and  $0.1\%$ , respectively.

The two important ingredients of precision in the present measurements are the accurate determination and subtraction of the background in the recoil proton spectra, and the accurate determination of the mean value of  $t$ . The procedures used have been described

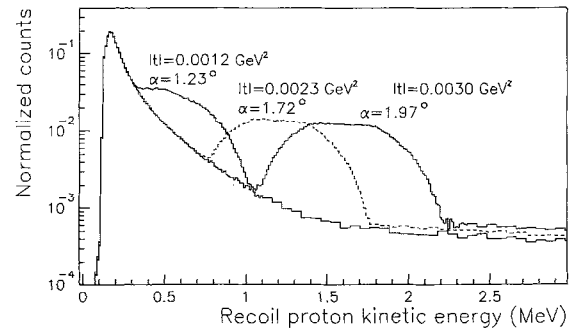


Fig. 3. The energy spectra of a detector at three recoil angles between one and two degrees for incident antiproton momentum  $p_{\text{lab}} = 5.6 \text{ GeV}/c$ . Note that the background on the low energy side of the three recoil peaks does not change appreciably.

in detail in Ref. [4]. Here we mention only the main points.

For  $|t| > 0.003 (\text{GeV}/c)^2$  ( $\alpha > 2^\circ$ ), proton recoil energies are larger than  $\sim 1.5 \text{ MeV}$ . In these cases the recoil peak, whose shape is due to the finite extensions of the interaction region and of the detectors, sits on top of a smooth and stable background which varies exponentially and which is nearly a factor 40 smaller than the peak. This background could be subtracted very reliably, and it is estimated [4] that the resulting uncertainty in the peak counts (usually  $> 100\,000$ ) is  $< 0.3\%$ . For  $|t| < 0.003 (\text{GeV}/c)^2$  ( $\alpha < 2^\circ$ ) the recoil energy is less than  $1.5 \text{ MeV}$  and the recoil peak sits on top of a background that increases rapidly as proton energy decreases (see Fig. 3). This background has several sources. Among them are detector noise, electronic noise, RF pickup and inelastic  $\bar{p}p$  reactions. As illustrated in Fig. 3, the background is very stable and can be determined accurately by comparing the recoil spectrum at one detector angle with that at an adjoining angle. As the recoil peak moves away with the change of angle, it reveals the almost exact form of the background under its former position. It is estimated that the error in the background subtracted recoil counts obtained by this method varies from  $0.3\%$  at  $|t| \approx 0.003 (\text{GeV}/c)^2$  ( $\alpha = 2^\circ$ ) to  $1.5\%$  at  $|t| \approx 0.0009 (\text{GeV}/c)^2$  ( $\alpha \approx 1^\circ$ ).

As indicated in Eq. (8), the determination of the mean value of the momentum transfer,  $|t|$  is equivalent to the determination of the mean value of the recoil energy  $T_p$ . An algorithm was developed to analyze the shape of the recoil peak to determine the mean

value of the recoil energy. Its accuracy was tested with Monte Carlo generated spectra which provided an accurate representation of the experimental spectra [4]. This procedure was used for all spectra with  $|t| > 0.003 \text{ (GeV/c)}^2$  ( $\alpha > 2^\circ$ ). However, it could not be used reliably for  $|t| < 0.003 \text{ (GeV/c)}^2$  ( $\alpha < 2^\circ$ ) for which the recoil peak sits on too steep a background. For such a case the recoil angle was determined from the known linear distance on the carriage between the detector at  $\alpha < 2^\circ$  and another detector on the carriage which was at  $\alpha > 2^\circ$  at the same time, and for which  $\alpha$  could be determined accurately by the procedure described before. It is estimated that recoil angles determined by either method have errors less than  $\pm 0.006^\circ$ , which correspond to errors in  $t$  which range from 1.1% at  $|t| = 0.0009 \text{ (GeV/c)}^2$  to 0.2% at  $|t| = 0.020 \text{ (GeV/c)}^2$ .

The procedures described above lead to background subtracted counts  $N(\alpha_i)$  and their errors (counting statistics and background uncertainty added in quadrature) for recoils in the different detectors at recoil angles  $\alpha_i$ . These counts are all normalized to the counts  $N(\alpha_0)$  in the fixed detector at  $\alpha_0 = 3.547^\circ$ , and are corrected for the measured small differences in the solid angles ( $\Delta\Omega$ ) of the different detectors. Note that these ratios

$$R(\alpha_i) = \frac{N(\alpha_i)/\Delta\Omega(\alpha_i)}{N(\alpha_0)/\Delta\Omega(\alpha_0)} = \frac{Ld\sigma(\alpha_i)/d\Omega}{Ld\sigma(\alpha_0)/d\Omega} = \frac{d\sigma(\alpha_i)/d\Omega}{d\sigma(\alpha_0)/d\Omega}, \quad (9)$$

and the corresponding errors  $\Delta R(\alpha_i)$  are independent of absolute luminosity  $L$ , and give *relative differential cross sections* as a function of  $\alpha$ , or equivalently of  $|t|$ , for a given momentum of the antiproton beam. (In actual practice, the antiproton beam momentum was scanned over the width of the charmonium resonance under investigation, but this variation was always less than 75 MeV/c, and for our purposes it was considered to be negligible.) These relative cross sections were then analyzed for the forward scattering parameters using the theoretical expressions in Eqs. (3)–(7), appropriately integrated over the finite geometry of the interaction region and the detectors. The best fit forward scattering parameters are determined by  $\chi^2$  minimization, with  $\chi^2$  defined as

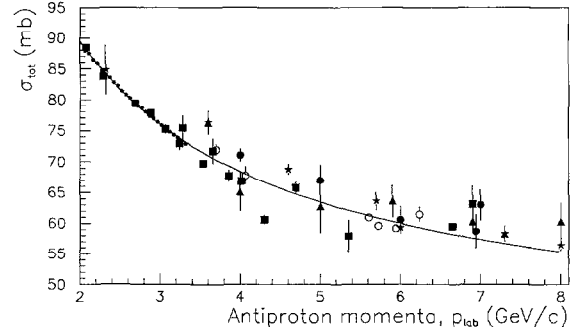


Fig. 4. World data on  $\bar{p}p$  total cross sections in the 2–8 GeV/c momentum range. Results of this experiment are shown as open circles. Results from the literature [5] are shown with filled symbols. The curve represents the best fit described in the text.

$$\chi^2 \equiv \sum_i ([R(\alpha_i)_{\text{exp}} - R(\alpha_i)_{\text{theo}}] / \Delta R(\alpha_i)_{\text{exp}})^2. \quad (10)$$

Since we have made measurements relatively deep into the Coulomb region,  $t \approx 0.0004 \text{ (GeV/c)}^2$ , we can analyze our relative differential cross sections for all three parameters  $\sigma_T$ ,  $b$  and  $\rho$ . The results of this analysis, which we call “ $\sigma_T$ -free” analysis are given in Table 1. We note that our results for the total cross sections (column 2 of Table 1) have 1%–2% errors but they appear to fluctuate by larger amounts. (See Fig. 4.) We also note that fluctuations in  $\sigma_T$  are accompanied by corresponding fluctuations in the values of  $b$  and  $\rho$ . This is, confirmed by the fact that the correlation coefficients between the parameters of the fits are found to be large. For example, the values are  $C(b, \sigma_T) = -0.56$ ,  $C(b, \rho) = -0.79$ , and  $C(\rho, \sigma_T) = +0.92$  at  $p_{\text{lab}} = 4.07 \text{ GeV/c}$ .

The large values of the correlation coefficients indicate that a substantial part of the fluctuations in the most sensitive parameter  $\rho$  are induced by fluctuations in  $\sigma_T$  and  $b$ . It is desirable to remove these correlation induced fluctuations in  $\rho$  by introducing sensible constraints on one of the other parameters. Usually this is done by fixing  $\sigma_T$  to values obtained from independent measurements or fits to them, and analyzing the differential cross section data only for  $b$  and  $\rho$ . For our second method of analysis we also follow this procedure.

In order to obtain the best estimates of  $\sigma_T$  we have fit the world data for  $\bar{p}p$  total cross sections [5] with the simple, and generally-used expression  $\sigma_T = A + Bp^n$

Table 1

Results for  $\bar{p}p$  elastic scattering parameters. The errors include systematic errors added in quadrature to all random errors.

$p_{\text{lab}}$ GeV/c	$\sigma_T$ -free analysis				$\sigma_T$ -fixed analysis			
	$\sigma_T$ mb	$b$ (GeV/c) $^{-2}$	$\rho$	$\chi^2/\text{df}$	$\sigma_T$ mb	$b$ (GeV/c) $^{-2}$	$\rho$	$\chi^2/\text{df}$
3.70	71.9(9)	12.6(4)	+0.018(14)	0.89	70.3	12.9(4)	+0.006(8)	0.90
4.07	67.8(15)	12.9(7)	-0.015(24)	0.60	68.0	12.8(7)	-0.007(12)	0.60
5.60	60.9(4)	12.6(2)	-0.047(7)	1.04	61.3	12.5(3)	-0.030(7)	1.04
5.72	59.5(6)	12.7(3)	-0.051(11)	1.13	60.9	12.2(4)	-0.018(8)	1.20
5.94	59.1(5)	13.0(2)	-0.063(8)	1.19	60.2	12.6(3)	-0.035(8)	1.26
6.23	61.5(12)	11.7(5)	-0.006(20)	0.42	59.4	12.2(6)	-0.029(10)	0.50

in various intervals of momentum, ranging from 2 GeV/c <  $p$  < 8 GeV/c to 2 GeV/c <  $p$  < 50 GeV/c, with and without including our values of  $\sigma_T$ , and obtained very consistent results. The data and the fit for the region 2 GeV/c <  $p$  < 8 GeV/c are shown in Fig. 4. The parameters for the best fit ( $\chi^2/\text{df} = 3.68$ ) are found to be  $A = 34.48(17)$  mb,  $B = 89.7(10)$  mb, and  $n = -0702(28)$ . The errors in the predictions of this fit are found to be typically  $\pm 0.16$  mb. Since no structure is expected in  $\sigma_T$  in the 2–8 GeV/c region, the large value of the best fit  $\chi^2/\text{df}$  is attributed to underestimates of errors in the old measurements. The realistic value of uncertainties in the best fit predictions is therefore estimated to be  $\pm 0.16\sqrt{\chi^2/\text{df}}$  mb =  $\pm 0.30$  mb.

For our second method of analysis we fix  $\sigma_T$  to the values predicted by the above fit, and listed in column 6 of Table 1. We then analyze the differential cross section data by the  $\chi^2$  minimization procedure described before by varying  $b$  and  $\rho$  only. The results of this “ $\sigma_T$ -fixed” analysis are also presented in Table 1. As expected, the large fluctuations in  $\rho$  values of the “ $\sigma_T$ -free” analysis are now much reduced, without

(GeV/c) $^{-2}$ , and  $\Delta\rho = \pm 0.0024$ .

The second source of systematic error is the uncertainty in the determination of  $t$ , because of systematic errors ( $\leq 0.2\%$ ) in detector energy calibration (thickness of the protective absorber on the surface of the  $\alpha$ -source, detector dead layer thickness, etc.). It is estimated that these uncertainties induce errors  $\Delta\sigma_T = \pm 0.07$  mb,  $\Delta b = \pm 0.14$  (GeV/c) $^{-2}$ , and  $\Delta\rho = \pm 0.0035$ .

We combine the above two contributions to systematic error in quadrature to obtain the estimate of final systematic errors in our  $\sigma_T$ -free analysis as:  $\Delta\sigma_T(\text{syst.}) = \pm 0.24$  mb,  $\Delta b(\text{syst.}) = \pm 0.23$  (GeV/c) $^{-2}$ , and  $\Delta\rho(\text{syst.}) = \pm 0.004$ .

For the  $\sigma_T$ -fixed analysis of Table 1, the uncertainty in the fixed value of assumed  $\sigma_T$  (typically  $\pm 0.3$  mb) constitutes an additional source of error for  $b$  and  $\rho$ . The estimated contributions from this source are  $\Delta b = \pm 0.08$  (GeV/c) $^{-2}$ ,  $\Delta\rho = \pm 0.005$ . These have also been included in the errors listed in Table 1.

In Fig. 5 we present the results for  $b$  and  $\rho$  from the present measurements (open circles) along with the published results [6] from the literature (filled sym-

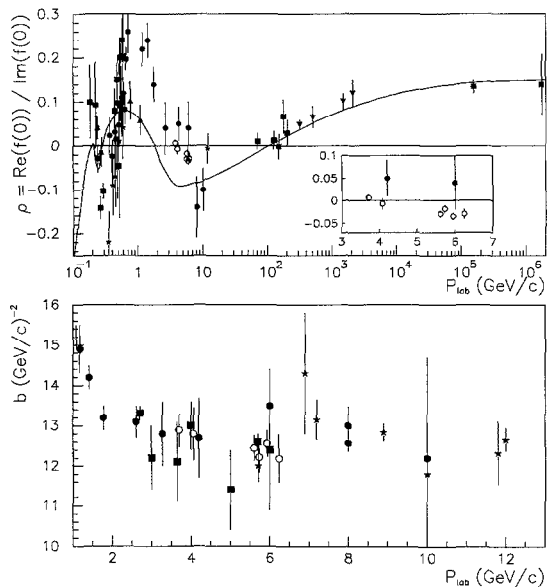


Fig. 5. (Top:) World data for the  $\rho$ -parameter, with the region covered by the present measurements also shown on an expanded scale in the inset. The solid curve is the dispersion relation prediction due to Kroll and Schweiger [8]. (Bottom:) World data for the  $b$ -parameter. In both panels results from the present measurements are shown as open circles. Results from the literature [6] are shown with filled symbols.

Dispersion relations predict the  $\rho$ -parameter in terms of  $pp$  and  $\bar{p}p$  total cross sections for  $\sqrt{s} > 2m_p$ , and parameters of those poles in the unphysical region ( $\sqrt{s} < 2m_p$ ) with which  $\bar{p}p$  can communicate. As is well known, for  $p_{\text{lab}} > 50 \text{ GeV}/c$  the predictions for  $\rho$  are completely determined by the measured  $\sigma_T$  and the contribution of the unphysical region to  $\rho$  is very small ( $< 0.02$ ). In contrast, as one goes to lower energies, the predictions become increasingly sensitive to the choice of relevant poles of the unphysical region and their parameters. In Fig. 5 we show the predictions of the latest dispersion relation calculation of Kroll and Schweiger. [8] The large errors in the existing experimental results for the  $\rho$ -parameter below 10 GeV/c provided few constraints to Kroll and Schweiger. They made their choice of the resonance poles and their coupling constants in the unphysical region to fit the LEAR data below 0.6 GeV/c, with the result that the existing data in the 1–10 GeV/c region were poorly fit. These predictions are now seen to be in clear disagreement with our precision results in the 3.5 to 6.2 GeV/c region. Hopefully, our results

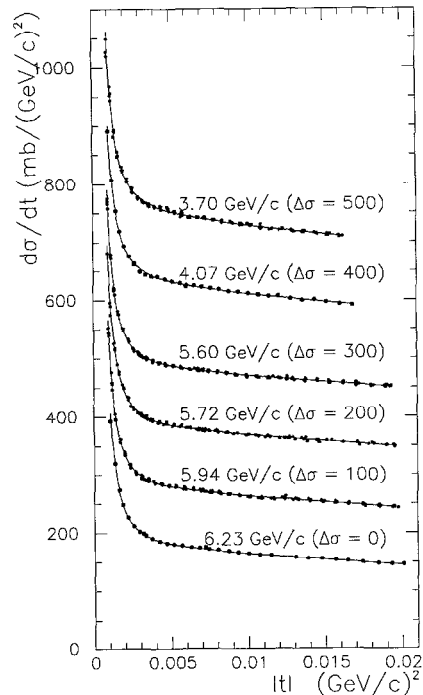


Fig. 6. Measured differential cross sections (increased as indicated by amounts  $\Delta\sigma$  (mb/(GeV/c)<sup>2</sup>) for display purposes) for six beam energies. The statistical errors are smaller than the size of the points. The solid line in each plot represents the fit to the data.

will motivate a new dispersion analysis and provide strong constraints for the choice of the poles and their parameters in the unphysical region. The success of our recoil detection technique also suggests that it can be used to great advantage in obtaining the much needed precision data in the region below 3 GeV/c, which should help pin down these parameters further.

The authors wish to acknowledge the help of the technical staff of the Fermilab Research Division and Accelerator Division in the design, fabrication, assembly and testing of the luminosity monitor. Special thanks are due to A. Beutler, L. Bartoszek, F. Carrera, H. Gusler, M. Kucera, and L. Bartoszek, F. Carrera, H. Gusler, M. Kucera, and M. Obrycki.

This research was supported in part by the U.S. Department of Energy, the US National Science Foundation, and the Istituto Nazionale di Fisica Nucleare of Italy.

**References**

- [1] R. Cahn, *Z. Phys.* C15 (1982) 253.
- [2] A.C. Melissinos and S.L. Olsen, *Phys. Rep.* 17 (1975) 77, and references therein.
- [3] E760 Collaboration, T.A. Armstrong et al., *Phys. Rev. D* 47, 3 (1993) 772.
- [4] S. Trokenheim et al., *Nucl. Instrum. Methods A* 355 (1995) 308.
- [5] Total Cross Sections for Reactions of High Energy Particles, LandoltBörnstein, New Series Vol I/12(a,b), ed. H. Schopper(1988).
- [6] For a compilation of the world data on  $b$  and  $\rho$ , see S. Trokenheim, Ph. D. dissertation, Northwestern University, 1995, unpublished.
- [7] P. Jenni et al., *Nucl. Phys. B* 94 (1975) 1; B 129 (1977) 232.
- [8] P. Kroll and W. Schweiger, *Nucl. Phys. A* 503 (1989) 865.